

Document downloaded from:

<http://hdl.handle.net/10251/161055>

This paper must be cited as:

Adam, JM.; Buitrago, M.; Bertolesi, E.; Sagaseta, J.; Moragues, JJ. (2020). Dynamic performance of a real-scale reinforced concrete building test under a corner-column failure scenario. *Engineering Structures*. 210:1-14. <https://doi.org/10.1016/j.engstruct.2020.110414>



The final publication is available at

<https://doi.org/10.1016/j.engstruct.2020.110414>

Copyright Elsevier

Additional Information

Dynamic performance of a real-scale reinforced concrete building test under a corner-column failure scenario

Jose M. Adam^{a*}, Manuel Buitrago^a, Elisa Bertolesi^a, Juan Sagaseta^b, Juan J. Moragues^a

^aICITECH, Universitat Politècnica de València. Camino de Vera s/n, 46022 Valencia, Spain

^bDepartment of Civil and Environmental Engineering, University of Surrey, GU2 7XH Guildford, UK

* Corresponding author. Tel.: +34 963877562; fax: +34 963877568.

E-mail address: joadmar@upv.es (J.M. Adam).

Abstract

The topic of robustness and progressive collapse of structures has attracted significant attention within the field of structural engineering recently. This is reflected by the rise in the number of scientific papers published in recent years as well as efforts in reviewing and developing codes for design. Although important numerical and experimental studies have been carried out to date simulating the sudden removal of columns to reproduce the possible consequences of an extreme event, most of these studies focus on subassembly systems and internal columns. Edge and corner columns are most vulnerable to accidental events. This paper gives the results of a test carried out on a purpose-built full-scale reinforced concrete building with a specially designed corner steel column used for the sudden column removal. The test was highly instrumented, involving 38 strain gauges, 38 displacement transducers and 2 accelerometers to monitor the vertical and lateral response. The results were used to analyse the dynamic performance of the structure after the sudden column removal as well as the alternative load paths (ALPs) mobilised during the test (i.e. flexural and Vierendeel action). The test showed a clear dynamic amplification of the strains and displacements (with high peaks); dynamic amplification factors (DAFs) were obtained accordingly. The load initially carried by the removed column was redistributed through the entire building system (not just the neighbouring columns). Tests on full-scale buildings, including the one described here, can be used to compile a database to validate codes and future numerical studies.

Keywords: *Experimental study; Extreme events; Progressive collapse; Robustness; RC structures; Corner columns.*

30 **1. Introduction**

31 Interest on structural robustness and progressive collapse has risen significantly in the last
32 twenty years [1] resulting into different research studies generally looking at testing of
33 subassembly of structural systems and numerical work with different level of sophistication [2–
34 5]. Extreme situations, also known as low-probability/high-consequence events, include, for
35 example: natural disasters (tsunamis, hurricanes, floods, etc.) or man-made hazards (e.g. terrorist
36 attacks, impacts or explosions). These events often cause local failure of some of the structural
37 members that can trigger a progressive collapse, with an inherent risk to human lives and property.
38 Some events with a high impact amongst the engineering community include the well-known
39 Ronan Point Apartment Block (London, 1968), the A.P. Murrah Federal Building (Oklahoma,
40 1995), the World Trade Center Buildings (New York, 2001) or, more recently, the Achimota
41 Melcom Shopping Centre (Acra, 2012), among others [6]. Events such as these have given rise
42 to the renewed interest of the scientific community and the international standards-issuing
43 authorities [1,7,8] in reviewing design clauses for robustness for traditional and novel forms of
44 construction.

45 The studies carried out in the past can be divided into two groups: a) those that aimed to
46 quantify and study the possible outcomes of extreme events (i.e. threat-dependent approaches)
47 [9,10]; and b) those that only attempted to minimise the consequences of a local failure, whatever
48 its cause (i.e. threat-independent approaches) and avoid the failure spreading to other elements in
49 the building [5,11,12]. Within this latter group, diverse numerical and experimental studies have
50 analysed the structural response of buildings subjected to column removal as recommended in
51 most current codes [13–15]. Although these studies included the possible causes of column
52 failures, including internal [16–23], external [2,16,24–31] and corner columns (e.g. [32–34]), few
53 studies have been done on corner column failures, even though these are the most vulnerable
54 columns in the structure (e.g. to impact). Existing tests on corner column removal focused on sub-
55 assemblies of frames or flat slab structures under monotonic loads applied by an actuator
56 [29,32,33,35–41]. Only tests by Xiao et al. [42,43] and Zhao et al. [44,45] considered complete,

57 but not full scale, structures and only the experimental study by Xiao et al.[42,43] was performed
58 under a real sudden loss of a corner column.

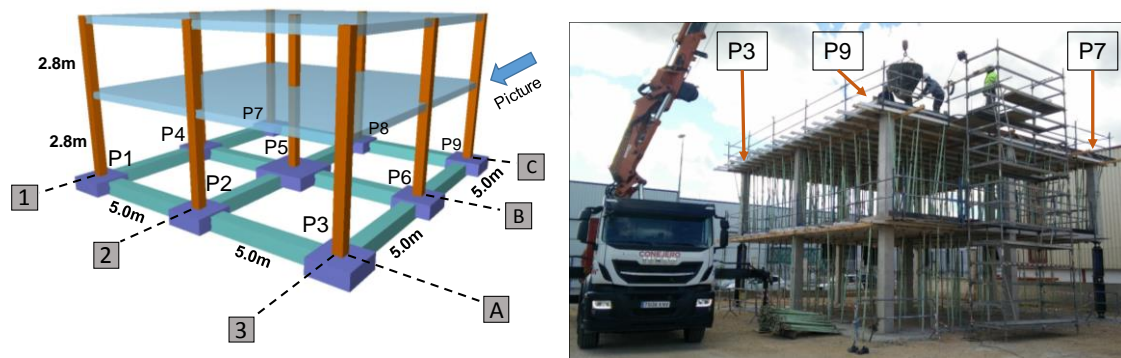
59 The most novel contribution from the present study is the testing of a two-story RC building
60 structure subjected to the sudden removal of a corner column with gravity loads defined in design
61 codes corresponding to a prescribed accidental load combination [13,14,46]. It should be noted
62 that tests in the literature were generally conceived to investigate the response to failure (including
63 the activation of large deformations) and therefore gravity loads applied in the specimens were
64 much higher than those specified in the building standards. Therefore the level of damage
65 observed in such tests is often higher compared to that predicted in typical design situations. As
66 discussed by Russel et al. [47] dynamic amplification is influenced by the level of damage which
67 in turn depends on the stiffness and the level of gravity loading applied in the structure. Hence, it
68 is debatable whether many of the tests in the literature are suitable to derive dynamic amplification
69 factors which are consistent with design assumptions.

70 Based on the limitation of existing test data mentioned above, the main objective of the
71 present work was to determine the dynamic performance of a full-scale RC building structure
72 under a corner-column failure scenario with loads, geometry and mechanical properties reflecting
73 design conditions. The second objective of this work was to analyse the test results to obtain a
74 better understanding of the various alternative load paths (ALPs) developed in the structure;
75 common tests on sub-assemblies can only mobilised a limited number of ALPs.

76 The paper is organized as follows: Section 1 includes the introduction, the aims and novel
77 aspects of the study; Section 2 describes the main characteristics of the building used in the test
78 as well as the main design considerations; Section 3 describes the test procedure and the
79 instrumentation adopted to monitor the structure; Section 4 gives the time-history results
80 (horizontal and vertical displacements, strains and accelerations) obtained during the test and
81 describes the final state of the structure after the sudden removal of the corner-column; Section 5
82 analyses and discusses the results; while Section 6 summarises the main conclusions and outlines
83 the possible direction of future lines of research.

84 **2. Description of the building**

85 The study was carried out on a full-scale RC building structure, specially built for this
86 purpose. Testing a full-scale specimen structure provides many benefits, since: 1) it allows certain
87 aspects to be considered that would be impossible to reproduce in sub-assembly tests, (e.g. 3D
88 effects, slab-column moment transfer, and the activation of different ALPs), 2) possible errors
89 due to scaling down can be avoided, and 3) a comprehensive monitoring system can be used
90 (including internal strain gauges at columns), which would be impossible to fit to an existing
91 building. The building was designed according to Eurocode 2 [48] for a high occupancy building
92 category (C1, C2 or C3) [49] with a dead load of 2 kN/m² and a uniformly distributed live load
93 of 3 kN/m² for the first and second slabs. The building had two floors with a free storey height of
94 2.8 m, four 5.0 m long squared bays, 20 cm thick flat slabs and 30 cm by 30 cm columns. Nominal
95 cover of columns and slabs was defined as 30 mm. The foundations consisted of isolated footings
96 connected by 40 cm squared beams. Fig. 1 shows a 3D view of the building, together with a photo
97 taken during its construction.

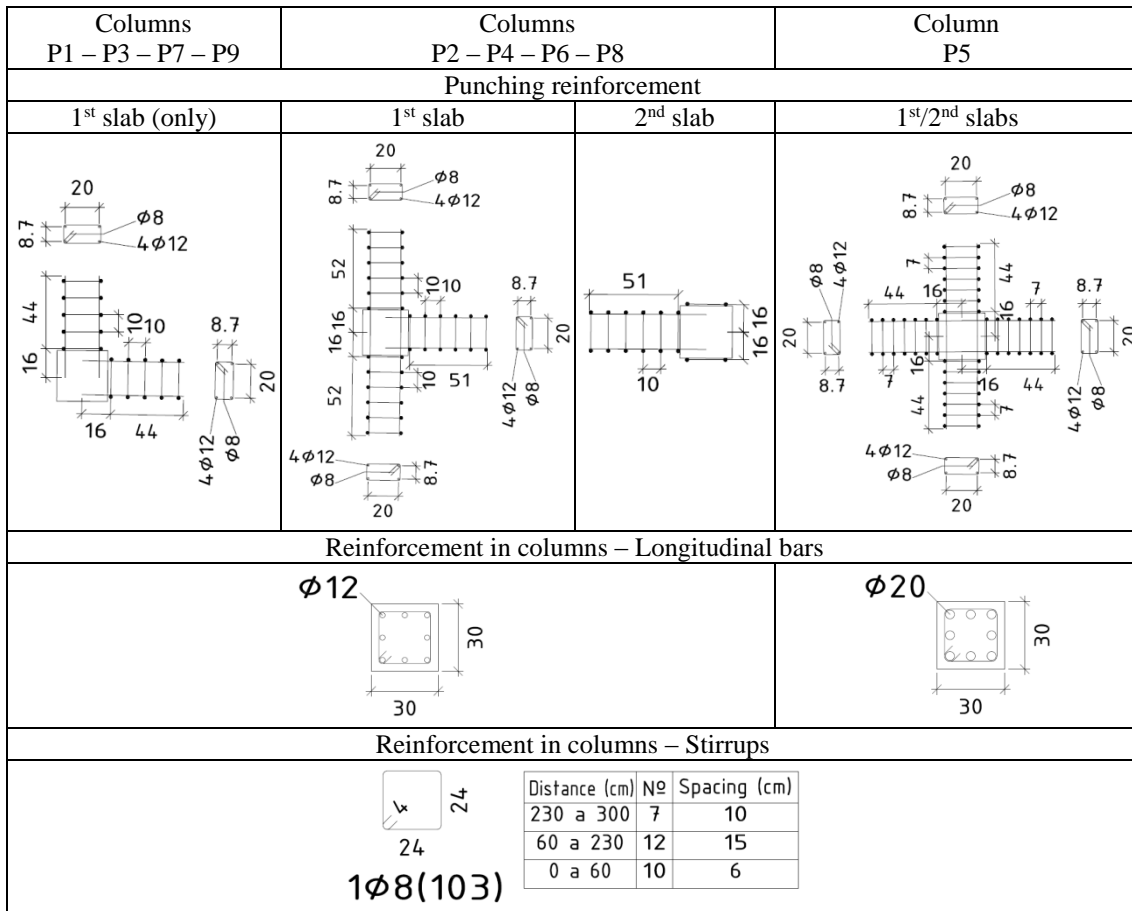


98
99 **Fig. 1. 3D view of the building structure.**

100 The building belongs to a consequence class 2a (Lower Risk Group) following Eurocode 1,
101 Part 1-7 [15], but it was categorised as a consequence class 2b (Upper Risk Group) as it is a test
102 which aim is to reproduce the behaviour of high occupancy and taller buildings. Subsequently the
103 building was also designed following the simplified method of tying forces and elements
104 (horizontal and vertical ties) [15]. A discussion of the origins and validity of the simplified tie
105 method can be found in [7]. All the structural members complied with the tying force

106 requirements except for column P5 for which the reinforcement was increased compared to the
107 other columns as shown in Fig. 3.





108 Figs. 2-3 summarize the final design of the RC building structure. For flat-slabs, a two-layer
109 reinforcement grid (top and bottom) was considered with 12 mm diameter bars spaced at 20 cm.
110 Extra reinforcement was adopted in the top layer, as shown in Fig. 2. Nominal concrete cover was
111 30 mm. The flat-slabs also had 30 cm wide edge RC beams (see Fig. 2) of the same thickness as
112 the slabs and introduced as a general adopted practice to withstand the edge moments and torsion.
113 Fig. 3 shows the slab punching reinforcement in the position of different columns, plus the column
114 reinforcement which was all designed using Eurocode 2 for the design loads give above. The
115 target characteristic compressive strength of the concrete (cylinder strength) for the entire
116 structure was 30 MPa ($f_{ck} = 30$ MPa) and control specimens were taken at the time of testing for
117 the different structural elements. The reinforcement characteristic yield strength was 500 MPa
118 ($f_{yk} = 500$ MPa).



122 **Fig. 3. Punching reinforcement and reinforcement in columns. Bar diameters in mm. Distances in**
123 **cm.**

124 The building was constructed in 51 days and the test was carried out 34 days after the concrete
125 was placed in the 2nd slab. The mechanical properties of the concrete were measured for different
126 concrete ages and elements (columns and slabs). The control specimens provided information on:
127 (i) compressive strength (4 cylinders per age and structural member, 30 cm height and 15 cm
128 diameter, following EN 12390-3); (ii) elastic modulus (3 cylinders per age and structural member,
129 30 cm height and 15 cm diameter, following EN 12390-13); (iii) tensile strength (3 Brazilian
130 cylinder tests per age and structural member, 30 cm height and 15 cm diameter, following EN
131 12390-6 and 3 flexural prismatic tests per age and structural member, 60 cm by 15 cm by 15 cm,
132 following EN 12390-5). The tensile strength was only tested for slabs. Table 1 shows the mean
133 values obtained.

134 **Table 1. Mechanical properties of concrete for columns and slabs.**

Mechanical property	Element	Age [days]	Results [MPa]	Test
Compressive Strength	Ground floor columns	57	32.2	
	1 st slab	43	30.5	
	1 st floor columns	42	33.2	
	2 nd slab	34	31.1	
Elastic Modulus	Ground floor columns	57	29275	
	1 st slab	43	28810	
	1 st floor columns	42	29403	
	2 nd slab	34	33119	
Tensile Strength	Ground floor columns	57	---	
	1 st slab	43	2.44	
	1 st floor columns	42	---	
	2 nd slab	34	1.83	
Flexural Strength	Ground floor columns	57	---	
	1 st slab	43	4.52	
	1 st floor columns	42	---	
	2 nd slab	34	4.08	

135

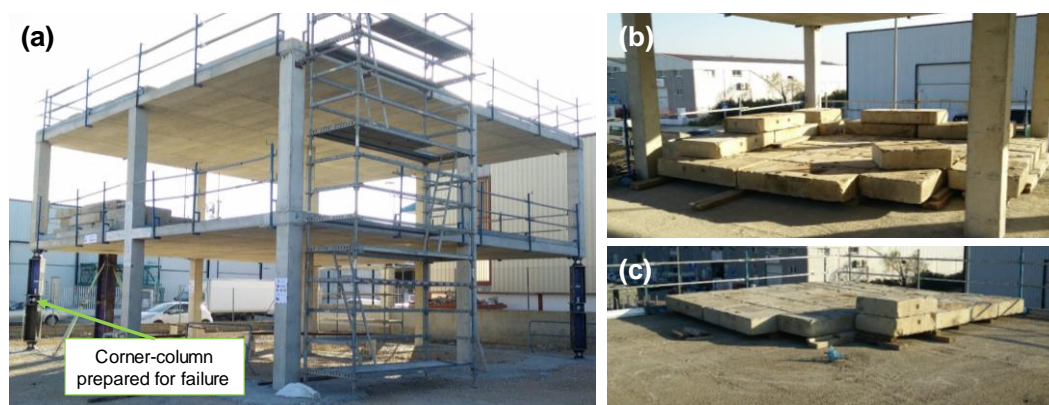
136 **3. Description of testing and monitoring**

137 **3.1. Failure scenario and gravity loads**

138 The local failure scenario consisted of the sudden removal of corner-column P3 (see Fig. 1).
 139 Corner columns are usually those most exposed and thus vulnerable to extreme events which
 140 could initiate progressive collapse. This scenario was thus deliberately chosen to study the
 141 capacity of a full-scale structure to seek ALPs and assessing the dynamic response.

142 As required in Eurocode [46], the total load considered for a combination of actions for
 143 accidental situations for a high occupancy building category C was $1.0 \cdot DL + 0.7 \cdot LL$, where DL is
 144 the dead load including that of the outside walls and LL is the live load. The GSA Guidelines [13]
 145 consider for accidental situations a total load of $1.2 \cdot DL + 0.5 \cdot LL$. In this work it was finally
 146 adopted a superimposed (additional) uniformly distributed load (ignoring the loads on the outside
 147 walls) equal to 4.9 kN/m^2 , which is the value required following the GSA Guidelines [13] which
 148 is slightly higher than the load required by Eurocode (4.1 kN/m^2) [46]. This load was reproduced
 149 by means of uniformly distributed concrete blocks arranged in the bays with the column removal

150 (the remaining bays had no superimposed loads). The blocks used for the superimposed load were
151 heavier than initially intended leading to a final load of 5.3 kN/m^2 . On the first floor, the weight
152 of a hypothetical outside wall was also considered by adding blocks at the edges; this was roughly
153 equivalent to a line load of 0.56 kN/m . Fig. 4 shows a photo of the finished building ready for
154 testing, with two views of the superimposed loads placed on each floor.



155

156 **Fig. 4. Details of the building (a) and the superimposed loads for the accidental situation on Floors**
157 **1 (b) and 2 (c).**

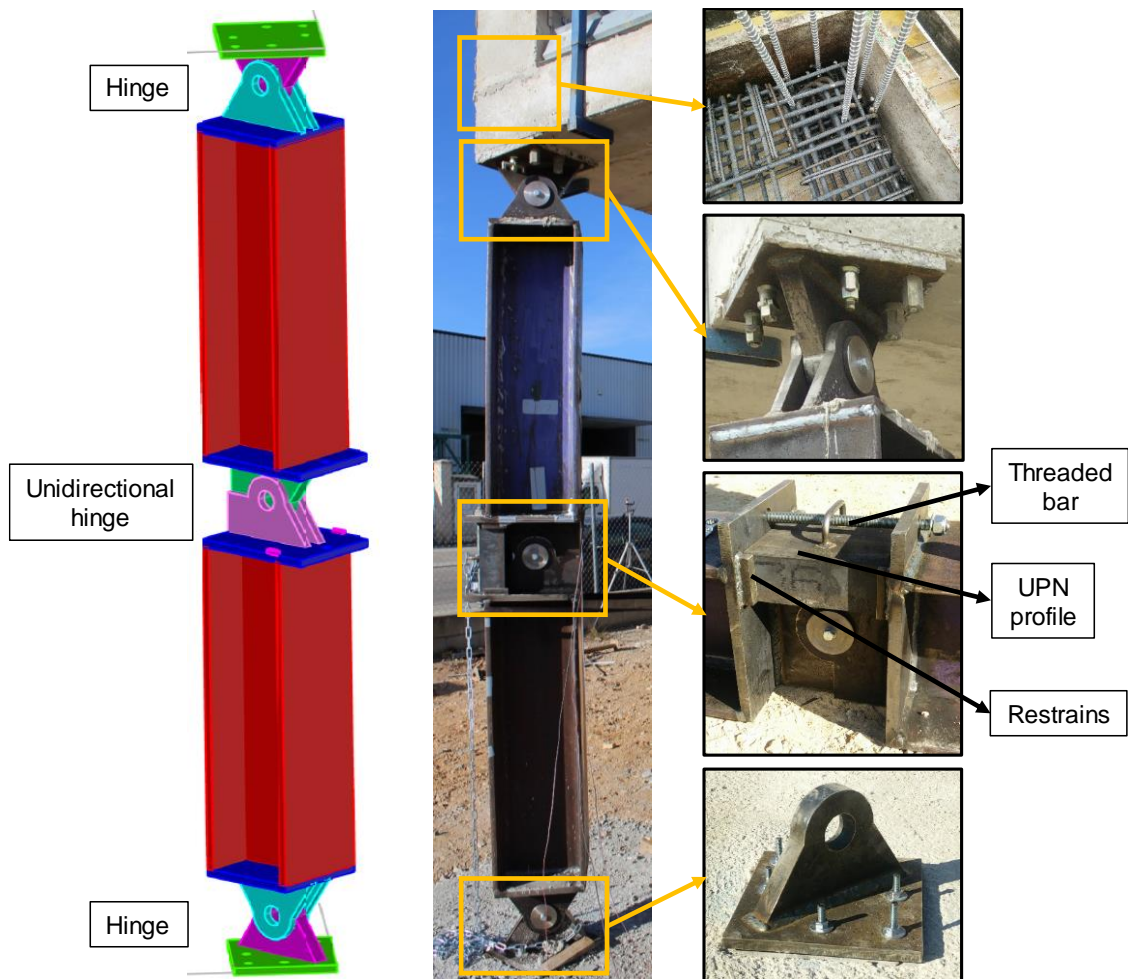
158 **3.2. Design of the corner-column for the failure scenario**

159 The sudden removal of column P3 on the first floor was achieved effectively using a steel
160 girder (HE-300B) fitted with three unidirectional hinges (see Fig. 5) which was specially designed
161 for this purpose. The intermediate hinge had a provisional block that allowed the column to
162 withstand the loads applied prior to the column removal. This hinge block allowed the movement
163 in a single direction and included a fitted U-shaped steel girder (UPN-240) with a pin restraint to
164 keep the girder in place during the building construction.

165 The upper hinge was anchored to the slab and upper column to mimic a conventional concrete
166 column, (i.e. the threaded bars used remained vertical prior to placing of the concrete of the slab
167 and second-floor column). The lower hinge was fixed to the foundations by means of threaded
168 bars and an anchor plate. All three hinges were turned 45° to allow the corner of the building to
169 move downwards freely. Details of the column design can be seen in Fig. 5, together with a view
170 of the completed column, details of the central hinge block and the connections between the upper
171 and lower parts.

172 The sudden column removal was achieved firstly by extracting the UPN girder (unblocking
173 the intermediate hinge) which was followed by a slight destabilisation of the column using a
174 forklift. Fig. 6 shows the moment just before the column was destabilised. For safety reasons an
175 additional column (unattached to the building structure as shown in Fig. 6) was placed next to the
176 removed column to prevent the total collapse of the structure.

177 The steel hinged column device adopted in the test was chosen over other alternatives such
178 as explosives or impact loads, which can be expensive and involve a certain amount of risk. These
179 alternative approaches can also generate vibrations and induced strains that can affect the results
180 obtained in the early stages of the tests. The column was also designed to be re-usable, i.e. after
181 the test it could be pushed back into place to return the slab to its original position and could be
182 used in subsequent tests in other parts of the building.



183

184

Fig. 5. Details of column design and installation.

Unblock: UPN profile

Destabilization



185

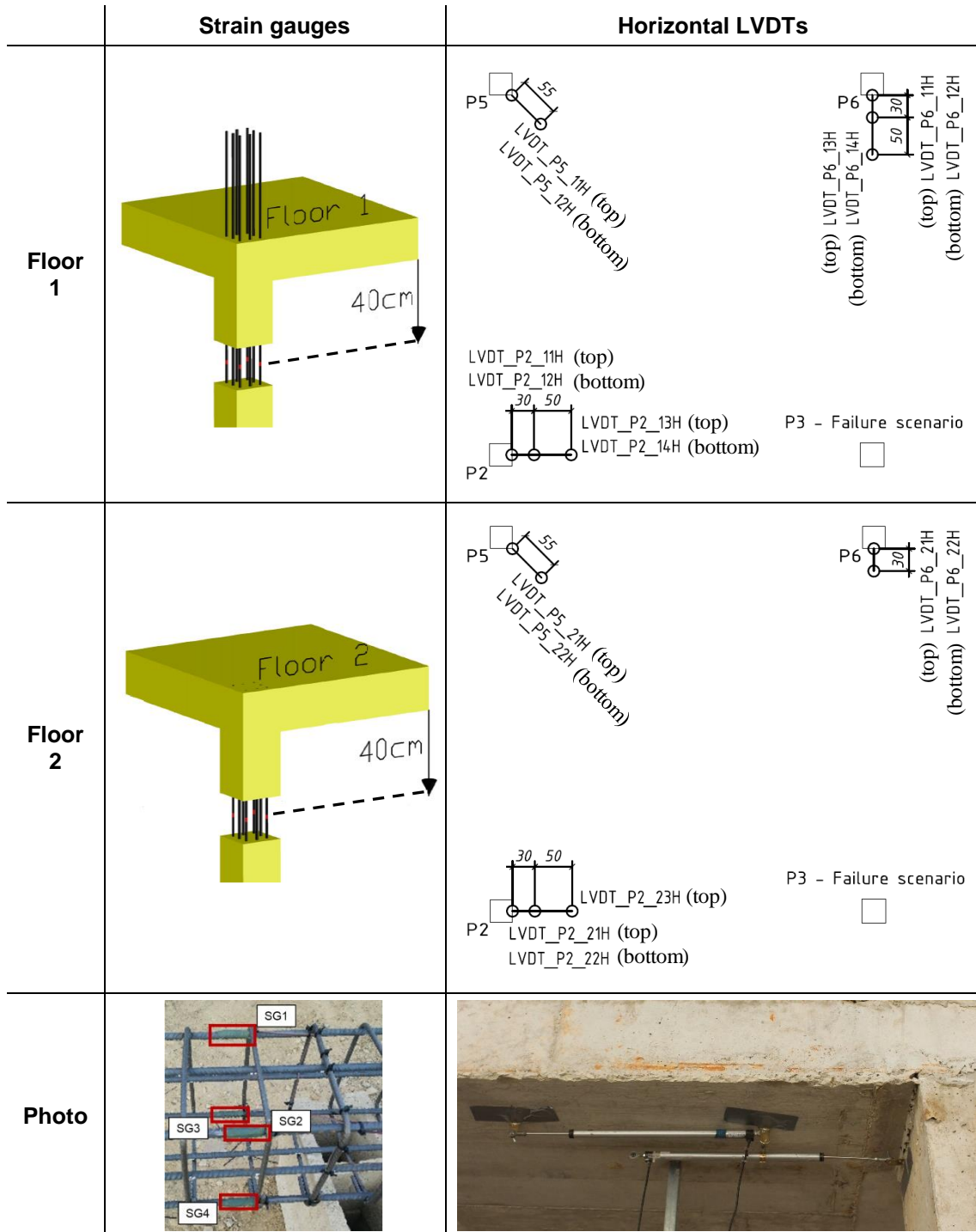
186

Fig. 6. Reproduction of the sudden failure of the column.

187 3.3. Monitoring

188 An extensive monitoring plan was designed with a total of 38 strain gauges, 38 LVDTs and
189 2 accelerometers. Four strain gauges were installed on the reinforcement bars on each of the first-
190 floor (P1, P2, P3, P5, P6 y P7) and second-floor columns (P2, P3, P5 y P6), while three were
191 fitted to the web and flanges of the HE-300B girder in the steel column (P3) (see Fig.7). These
192 were labelled following the pattern SG_Column-XY, where X indicates the floor (from 1 to 2)
193 and Y indicates the number and position of the strain gauge (from 1 to 4).

194 Seventeen of the 20 LVDTs placed horizontally on the top and bottom slab surface were used
195 to measure bending in the slab-column joint (see Fig.7); these were labelled following the pattern
196 LVDT-Column-XYZ, where X indicates the floor, Y indicates the number and position of the
197 LVDTs, and Z adopts letters H or V which means horizontal or vertical, respectively. Three
198 horizontal LVDTs measured the building drift towards the failed column on Floors 1 and 2 (see
199 Fig. 8).



200

Fig. 7. Position of strain gauges and horizontal LVDTs.

201

Eighteen LVDTs measured vertical displacement at different points in the structure. Eleven

202

were used to measure slab deformation at a distance of three times the effective slab depth from

203

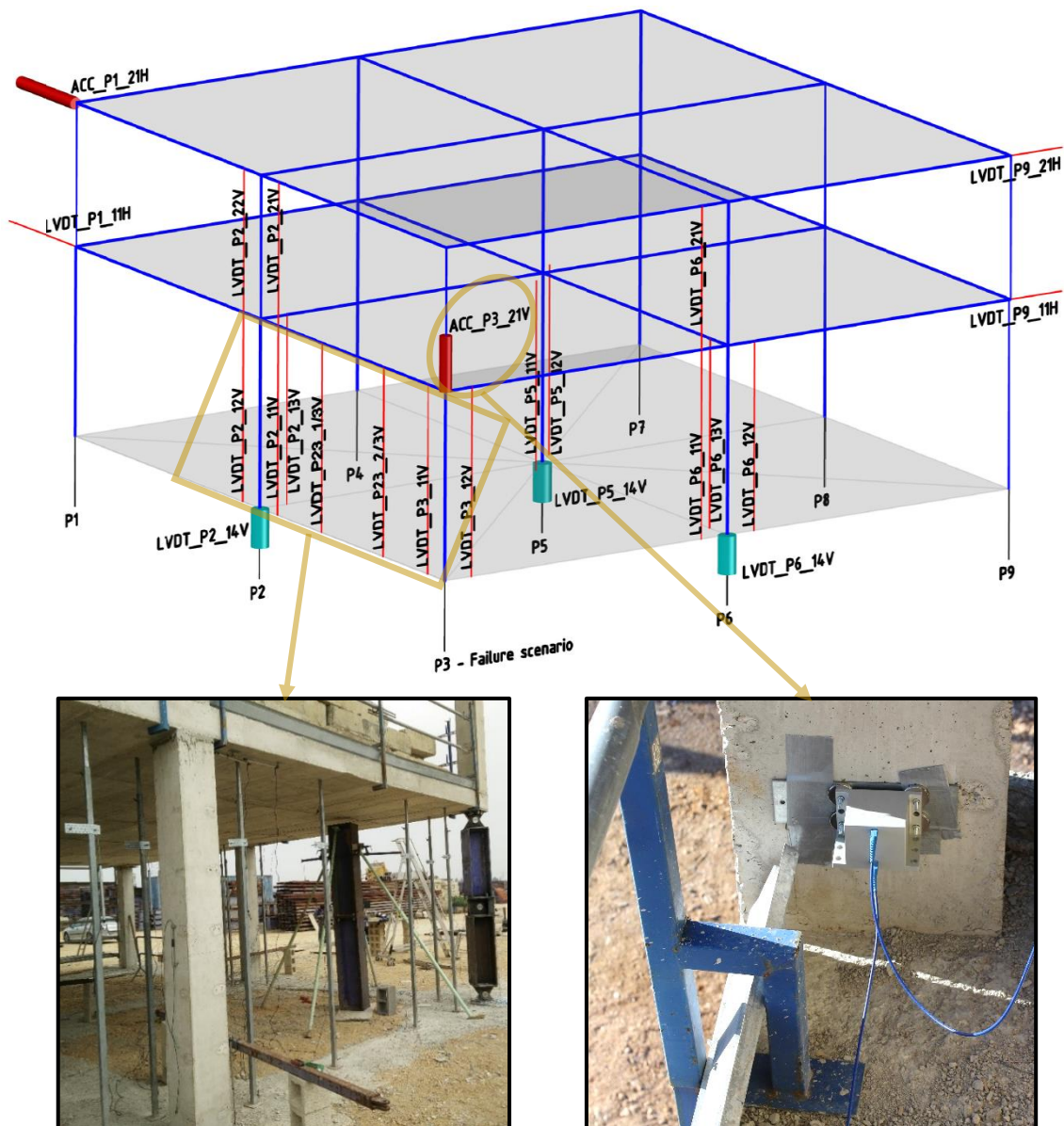
the columns face (47cm). Two vertical LVDTs measured vertical structural displacement at 50

204

cm from the failed column (P3) and two others the deformation of the P2-P3 alignment (1/3 and

205 2/3 of the span length; labels LVDT_P23_1/3V and LVDT_P23_2/3V respectively). Three
206 vertical LVDTs (green cylinders in Fig.8) recorded the time-history settlement of the foundations
207 of columns P2, P5 and P6.

208 The vertical accelerations generated during the test in the upper section of the failed column
209 and horizontal accelerations over P1 towards P3 were measured by two fibre optic accelerometers
210 (red cylinders in Fig.8).



211
212

Fig. 8. Position of vertical LVDTs and accelerometers.

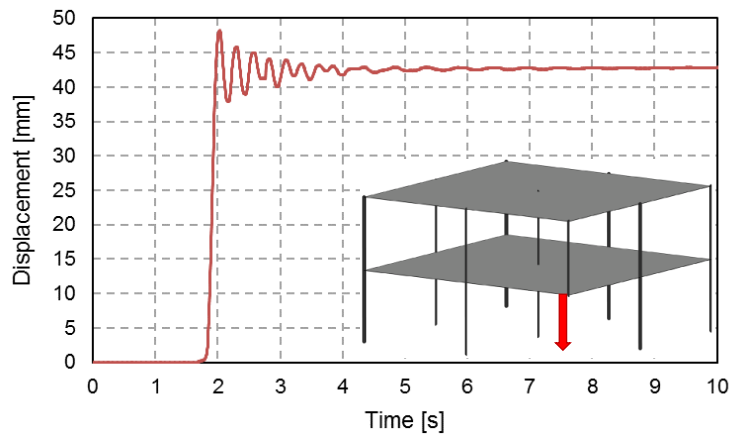
213 A high-capacity 78-channel data acquisition system was used to monitor the deformation and
214 displacement sensors at a rate of 200 measurements per second (200Hz frequency). The fibre
215 optic sensors used an optical sensing interrogator operated at the same frequency.

216

217 4. Time-history results and final state of the structure

218 4.1. Vertical displacements

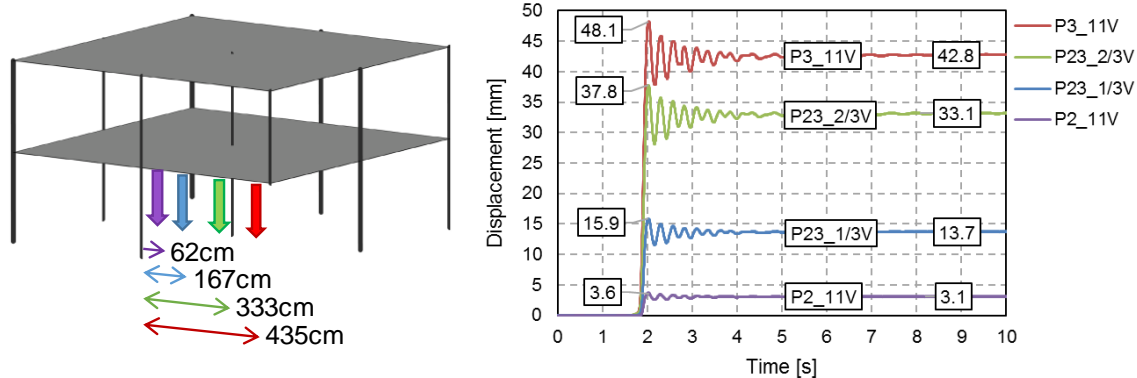
219 Fig. 9 shows the time-history of the vertical displacement of one of two LVDTs close to the
220 failed column P3. Both sensors (P3_11V and P3_12V) showed similar values, with a maximum
221 descent of 48.1mm and stabilised at 42.8mm two seconds after the sudden column removal.



222

223 **Fig. 9. Vertical displacement in the position of the failed column.**

224 The deformation profile between P2 and P3 was recorded by four LVDTs (P2_11V,
225 P23_1/3V, P23_2/3V and P3_11V, see positions in Fig. 8). Fig. 10 gives the results obtained
226 before, during and after the removal of P3. The positions of the sensors can be seen, together with
227 a time-history graph of vertical displacements with time. Peak displacements and residual
228 displacements are also given. The ratio between peak and residual values ranges from 1.12
229 (P3_11V) to 1.16 (P2_11V).

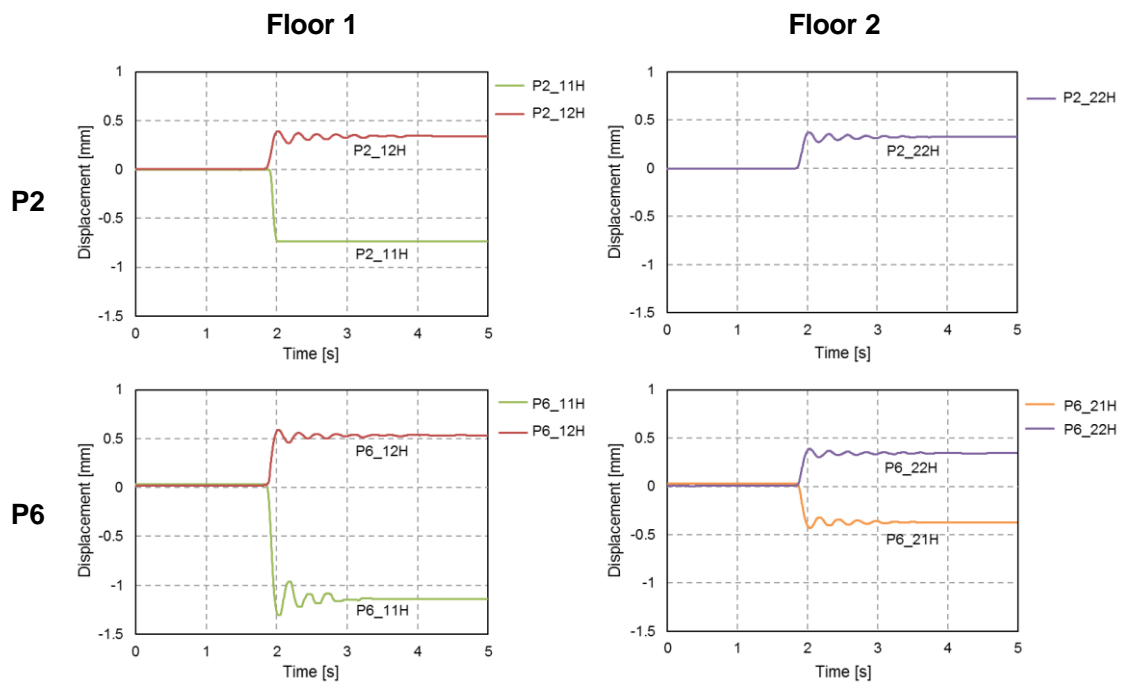


230
231 **Fig. 10. Vertical displacements between columns P2 and P3.**

232 **4.2. Horizontal displacements**

233 Horizontal displacement was measured by the LVDTs in order to investigate: a) bending
234 deformations (flexural and Vierendeel actions) and in-plane deformations (membrane action)
235 using sensors placed on column-slab joints; and b) drift of the structure after the sudden removal
236 of column P3 using sensors referenced to a fixed point outside the structure.

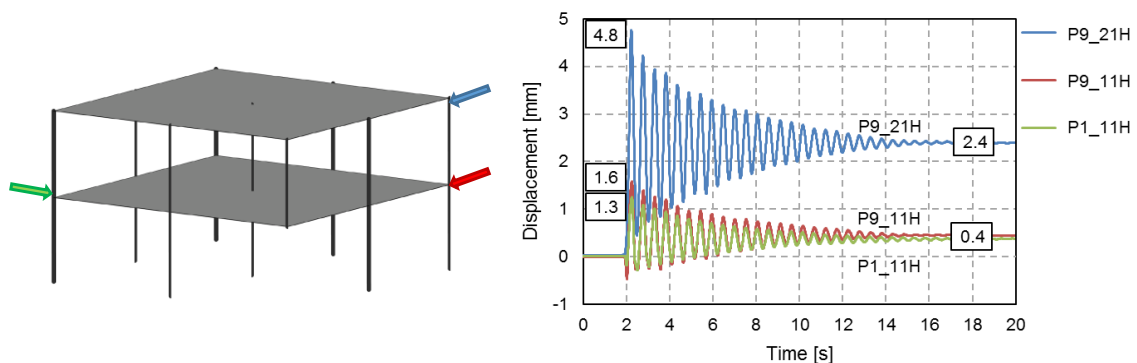
237 Fig. 11 shows the relative horizontal displacement time-history results for the seven LVDTs
238 on column-slab joints around columns P2 and P6 on the first and second floors (P2_11H, P2_12H,
239 P2_22H, P6_11H, P6_12H, P6_21H and P6_22H, see positions in Fig. 7). The data from sensor
240 P2_21H is not shown as the sensor was faulty during the test. The results show that the upper face
241 of the slab is in tension while the lower is under compression, with tensile deformation higher
242 than compression deformation due to localised slab cracking. Slightly asymmetric behaviour can
243 also be seen in the first-floor structure, where the sensors close to P6 recorded larger
244 displacements than those around P2, although those on the second floor all gave similar values.



245

246 **Fig. 11. Horizontal displacements on slabs near columns P2 and P6 on first and second floors.**
 247 **Positive values represent compression displacements.**

248 Fig. 12 shows the time-history of the drift of the building (P1_11H, P9_11H and P9_21H, see
 249 positions in Fig. 8). P1 and P9 gave similar results on the first floor, with a residual difference
 250 value of approximately 0.4 mm, and slightly different peak values, with P9 showing the higher
 251 horizontal displacement (1.6 mm) than P1 (1.3 mm). The mean values are much higher on the
 252 second floor, with a peak of 4.8 mm and residual value of 2.4 mm. In this case, the ratio between
 253 peak and residual values ranges from 2.0 (P9_21H) to 4.0 (P9_11H).



254

255 **Fig. 12. Drift of the building after the sudden removal of the corner column. Positive values**
 256 **represent displacements towards P3, as indicated by the arrows.**

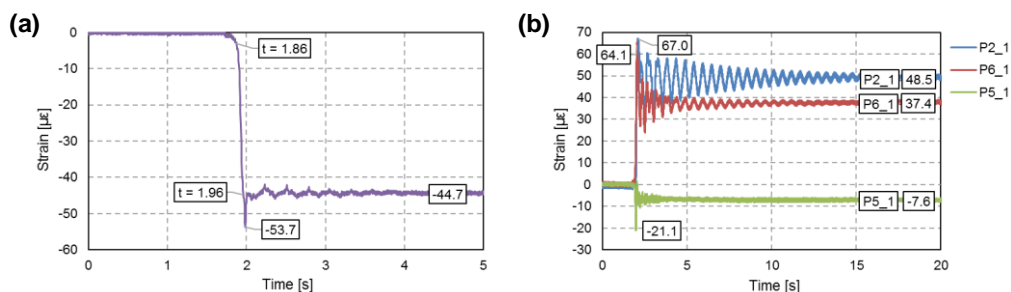
257

258 **4.3. Strain in columns**

259 P3 was monitored by 3 strain gauges to measure: a) column load before the sudden removal
 260 and b) column unloading time. Fig. 13a gives the mean values of P3, with an unloading time of
 261 approximately 0.1 s and 44.7 $\mu\epsilon$ of elongation (140 kN).

262 The columns nearest P3 (P2, P5 and P6) were also monitored. Fig. 13b shows the mean values
 263 of the four strain gauges fitted to these columns on the first floor (represented with the following
 264 codes P2_1, P5_1 and P6_1) to measure the increased axial force on these columns. It can be seen
 265 that P2 and P6 absorb high compression forces (i.e. shortening strains), while the load in P5
 266 remains fairly constant with a small unloading. Residual values of the load increments are 37.4
 267 $\mu\epsilon$ (104 kN) and 48.5 $\mu\epsilon$ (135 kN) in P6 and P2 respectively, showing increased compression
 268 values close to the unloading values of P3 (140 kN). As explained in Section 5, the higher load in
 269 the neighbouring P2 and P6 columns can be explained by the unloading of other columns due to
 270 the global eccentricity of the load in the building (in the direction P5-P3) after column removal.

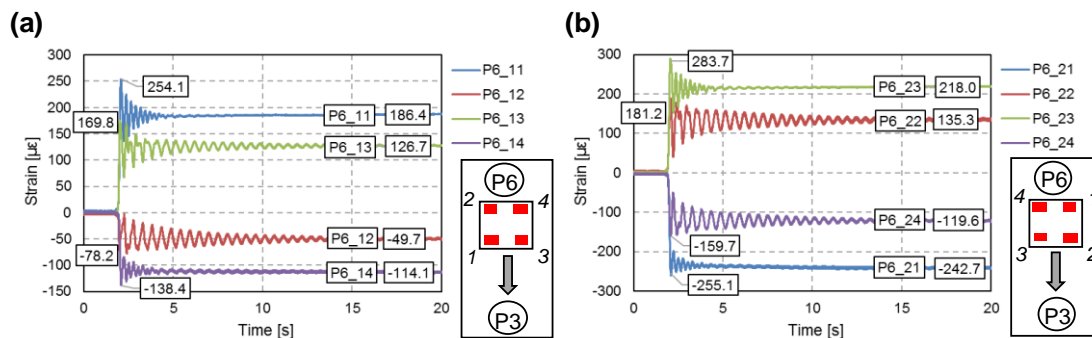
271 P2 (48.5 $\mu\epsilon$) showed higher residual compression deformation increments than P6 (37.4 $\mu\epsilon$),
 272 but the same did not happen with the peak values, (67.0 $\mu\epsilon$ and 64.1 $\mu\epsilon$ for P2 and P6,
 273 respectively). This can be explained by the more severe cracking and deformation of the zone
 274 close to P6 than around P2 (see Fig. 11 and Section 5), reducing the stiffness in this zone on
 275 reaching maximum load and thus re-distributing part of the load to stiffer regions. The ratio
 276 between peak and residual loads, which depends largely on load distribution during the dynamic
 277 action, had values ranging from 1.38 to 1.71 in P2 and P6 respectively.



278 **Fig. 13. Mean first-floor strain gauge value for columns: (a) P3, and (b) P2, P6 and P5. Positive**
 279 **values indicate shortening and negative indicates decompression.**
 280

281 Besides higher axial forces, the sudden column removal also caused significant variations in
 282 the column bending moments including P2 and P6. These bending moments were assessed by
 283 analysing the deformation data from the four strain gauges 40 cm below the slab on the upper
 284 section of the columns. These results confirm the contribution of flexural and Vierendeel action
 285 similar to that reported for frame buildings [50,51].

286 Fig. 14 shows the deformation recorded by the strain gauges in P6 at the first and second
 287 floors (Figs. 14a and b). The two strain gauges on the side of P6 closest to P3 give compression
 288 deformation increments (shortening), while the other two are in tension (elongation). These values
 289 indicate the presence of large bending moments leading to an overall rotation of the slab-column
 290 joint towards P3. These values are much higher than those recorded for axial force deformation
 291 (see Fig.13b), reaching a peak of 283.7 $\mu\epsilon$, denoting the high flexural deformation of the slab-
 292 column joint.

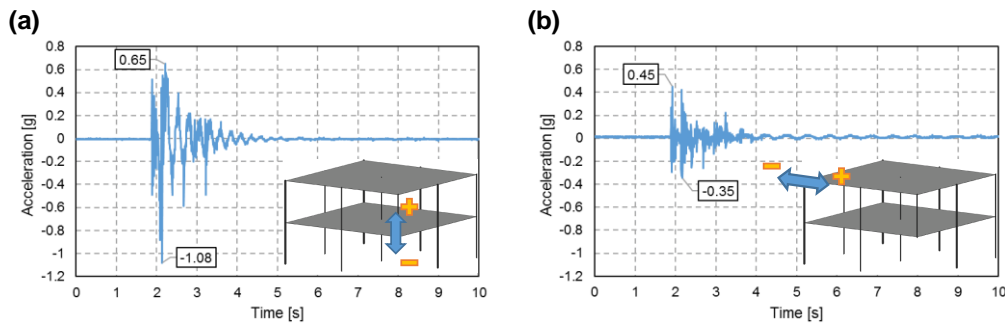


293
 294 **Fig. 14. Strain measures in P6 on the first (a) and second (b) floors. Positive values represent**
 295 **shortening.**

296 4.4. Acceleration

297 The acceleration measured above the removed column is shown in Fig. 15. The vertical
 298 acceleration is close to free fall with a peak value of 1.08 g followed by the high frequency
 299 oscillation phase. These results demonstrate that the sudden removal of the corner column was
 300 successfully reproduced in the test. The results also show the dynamic response of the structure,
 301 with a clear recoil, reaching a deceleration of up to 0.65g. Fig 15b shows the horizontal

302 acceleration of the structure at the highest point of P1, which is significant, reaching values of
303 0.45 g towards the removed column and 0.35g in the opposite direction.



304

305 **Fig. 15. Vertical (a) and horizontal (b) acceleration in column P3 (1st floor) and column P1 (2nd**
306 **floor), respectively.**

307 4.5. Residual damage after the test

308 There was no extensive cracking in the structure before and after removing the column; only
309 the upper slab surface around P2 and P6 were affected, as confirmed by the results given in Fig. 11.
310 Flexural cracks in the slab were visible near the column-slab connection as shown in Fig. 16. At
311 the end of the test, for safety reasons, P3 was pulled back into its original position by a cable until
312 the central hinge re-blocked; flexural cracks closed consequently.



313

314 **Fig. 16. Final state of the removed column and detail of cracking on P2 slab-column joint (1st floor).**

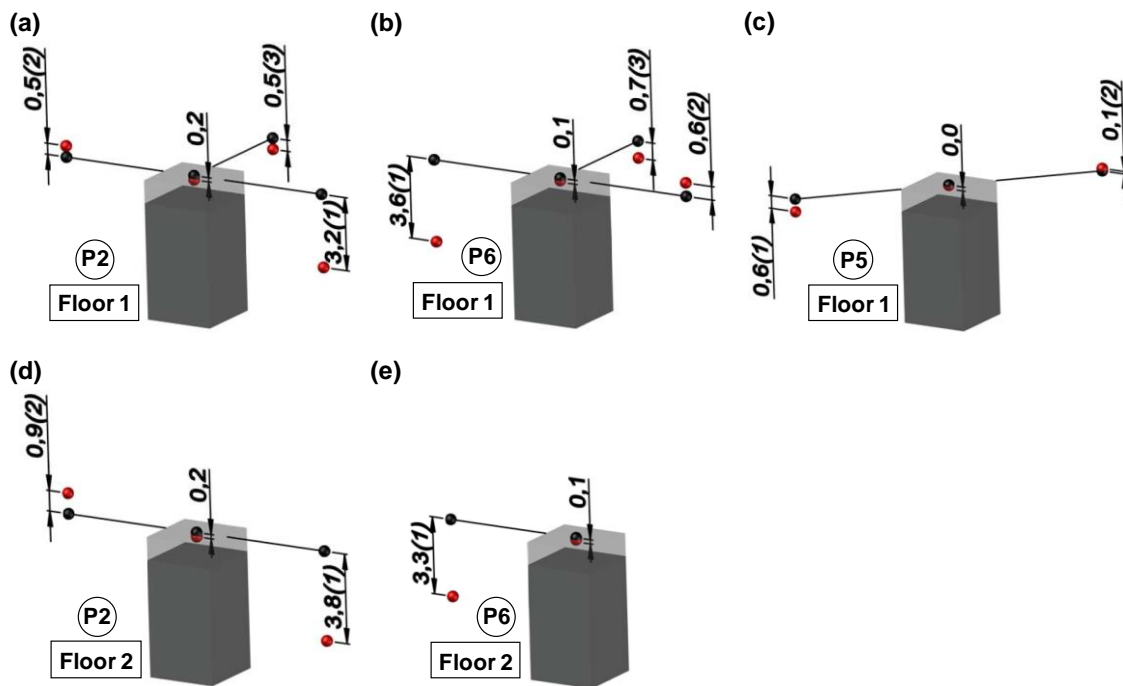
315 **5. Analysis and discussion of results**

316 This section deals with: a) slab flexural deformation around the neighbouring columns (P2,
317 P5 and P6); b) the re-distribution of the load originally carried by P3; c) the overall behaviour of
318 the structure and the main ALPs after the sudden removal of the corner column; and d) a
319 description of the linear static numerical analysis carried out to evaluate the dynamic
320 amplification factors (DAF) defined in the DoD guidelines [14].

321 **5.1. Deformability of slabs around adjacent columns**

322 Fig. 17 gives the residual vertical displacements around columns P2, P5 and P6 and represents
323 the situation before (black spheres) and after (red spheres) the column removal. Each sphere is
324 separated from the column face by a distance of three times the effective slab depth (47cm). The
325 position at which the measurements were taken is given in brackets, with reference to Fig. 8, next
326 to the vertical displacement, in addition to the column number and floor. The results clearly show
327 that the nodes turned towards the position of P3, with a pronounced drop at the closest point to it
328 and a slight rise at the opposite point. This is a typical situation of a column-slab connection
329 subjected to moment transfer.

330 The data supplied here will be subjected to a more in-depth analysis using simplified corner
331 column failure methods in order to determine the dynamic punching demand and resistance.
332 Flexural rotations vary significantly close to the column whereas further from the column they
333 become fairly constant. The constant value of the slab rotation, which can be obtained from the
334 measured data, is the one of real interest for assessing punching resistance. In any case, the test
335 shows that punching shear was not critical for the accidental load combination investigated.



336

337 **Fig. 17. Residual displacements after the sudden removal of column P3 around columns P2 (a and**
 338 **d), P6 (b and e) and P5 (c). Units in mm. Scale factor of 100 for vertical displacements.**

339 **5.2. Analysis of the load redistribution after column removal**

340 The results obtained show that the sudden unloading of the corner-column (P3, initially
 341 carrying 140 kN) resulted in a large increase of the residual axial load in the neighbouring
 342 columns. The value of the load increase (135 kN and 104 kN for P2 and P6 respectively) is similar
 343 to the load on the corner-column before it was removed. This is different to column removal
 344 scenarios for internal columns for example where only a fraction of the load carried by the column
 345 is transferred to the neighbouring columns after column removal.

346 In this test it is shown that the load in P3 is transferred to P2 and P6 with a significant
 347 additional axial load and moment transfer due to the unloading of other columns. This response
 348 is due to the global eccentricity of the load and the asymmetry of the building after column
 349 removal. To further illustrate this behaviour, Table 2 gives the mean deformation and residual
 350 axial force increments (calculated from the strain increments measured by the 4 strain gauges on
 351 each column) of P3, P2, P6, P1, P5 and P7. All the first-floor columns except P2 and P6 are shown
 352 to experience a reduction of the axial loads.

353 If P9 is considered to reduce its load by a similar amount to P1, and if the reduced load on P4
 354 and P8 is between the reduction on P1 and P7, the total axial forces (or vertical reactions) of the
 355 structure are in equilibrium. It can also be seen that the reduced load on P1 is even slightly higher
 356 than the reduction of P5 (closer to P3), which, together with the large load increases on P2 and
 357 P6, underlines the importance of the outside frames working with the flexural and Vierendeel
 358 beam actions. These global effects and the contribution of the different floors to the search for
 359 ALPs could not have been considered had the test been made on a sub-assembly.

360 **Table 2. Analysis of the load redistribution after the sudden removal of column P3. Shortening strain**
 361 **increments are positive.**

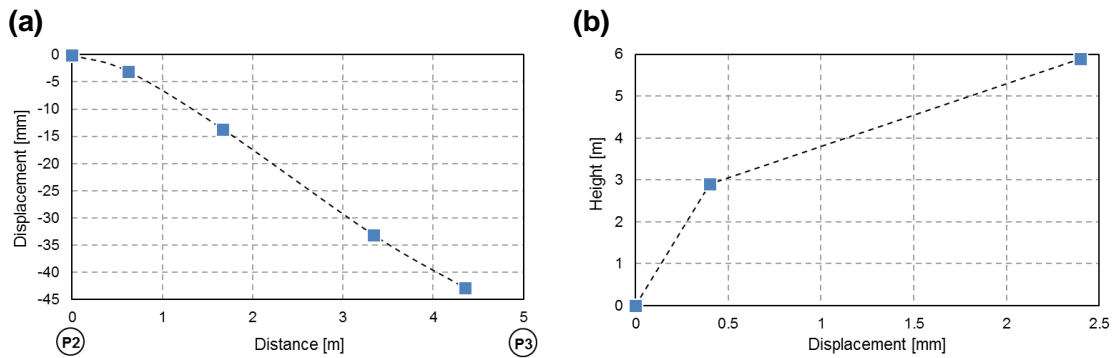
Column	Residual mean strain [$\mu\epsilon$]	Axial force increment [kN]
P3 (removed)	-44.7	-140
P2	48.5	135
P6	37.4	104
P1	-8.9	-25
P5	-7.6	-21
P7	-3.6	-10

362

363 5.3. Analysis of ALPs of the structure

364 The main ALPs were analysed for the corner-column failure scenario tested. After this type
 365 of event there are different possible ALPs [1]: (i) flexural or slabs acting as cantilevers, (ii)
 366 Vierendeel beam, (iii) tensile membrane action, (iv) compressive membrane action and (v) others
 367 such as the possible contribution of partitions or secondary trusses. The compressive membrane
 368 effect (iv) and contribution of partitions (v), are not applicable to the case under study since the
 369 former is not possible in corner-column failure scenarios and partitions were not considered in
 370 the study. Flexural action was obviously present in the test carried out, since the corner bay
 371 remained partially functioning as a cantilever (see Figs. 11-16). The Vierendeel beam mechanism
 372 was also activated. As already mentioned, Vierendeel behaviour can be proved by the deformed
 373 shape of the structure (columns experienced severe flexural deformations and slabs had a double-
 374 curvature deformation as shown in Fig. 18). Fig. 18a shows the vertical deformed shape of the
 375 first-floor slab between P2 and P3. The results show that deformation is not only due to flexural
 376 or cantilever action, but that the Vierendeel beam effect is also significantly present.

377 Fig. 18b shows the horizontal deformation of P9 as representative of the drift of the structure.
 378 The deformation is not uniform, but is approximately five times greater on the second than the
 379 first floor, and also indicates the existence of the Vierendeel beam mechanism, which reduced the
 380 horizontal deformation on the first floor. It should be noted that this mechanism also requires the
 381 bending capacity of the slab-column joints which is limited due to punching and moment transfer.



382

383 **Fig. 18. Vertical residual displacement of the first floor between columns P2 and P3 (a) and**
 384 **horizontal residual displacement of column P9 (b).**

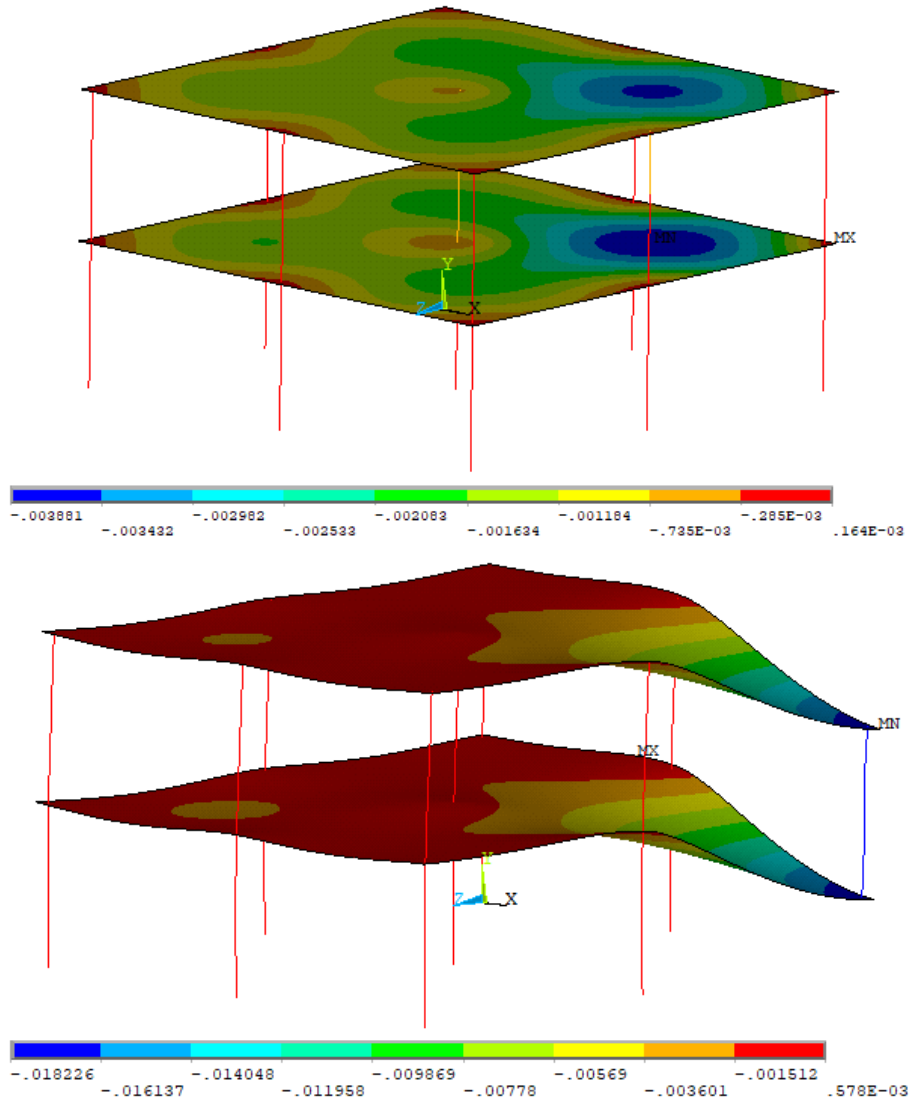
385 Membrane action (compressive and tensile) was not activated in the test. Compressive
 386 membrane action due to restraint slab dilatancy from cracking was not possible, other than locally
 387 at slab-column joints, due to the lack of in-plane restraint at the edges of the bay of the column
 388 removal. This situation is different for internal column removal where in-plane restraint takes
 389 place. Tensile membrane action which may be present in corner-column failures, it is often
 390 considered as an extra reserve that comes into play after the activation of flexural and Vierendeel
 391 beam mechanisms [37]. The deformation of the slab after column removal was small (48 mm near
 392 P3); as an order of magnitude this value is near the prescribed limit of span $L/250$ imposed by
 393 Eurocode 2 [48] to avoid functionality issues (general utility and appearance). This value is
 394 considerably lower than the usual range where tensile membrane action is activated; snap-through
 395 just before the activation of tensile membrane action occurs at vertical deflections of the order of
 396 the thickness of the slab [52–54]. It can be concluded that the main ALPs in the test were flexural
 397 and Vierendeel actions.

398

399 **5.4. Evaluation of Dynamic Amplification Factors (DAFs)**

400 The international recommendations for the design of robust buildings (e.g. US Department of
401 Defence (DoD) [14]) allow linear static analysis as a simplified calculation method as part of the
402 Alternative Load Path method, without considering more complex aspects such as mechanical
403 non-linearities and dynamic (inertial) effects. However, the calculations must include dynamic
404 load amplification factors (DAFs) to cover any effects not taken into account; these are embedded
405 in the “load and dynamic increase factors” in [14].

406 The use of a linear static approach in the DoD guidelines is restricted to structures without
407 “structural irregularities” as well as irregular structures in which the estimated demand-capacity
408 ratio from the linear analysis is less or equal than 2.0. Therefore this approach seems suitable for
409 the structure tested in this work. In the present study a linear static analysis was performed using
410 ANSYS software [55] to compare the experimental and numerical results in order to evaluate the
411 DAFs, as has been done in previous studies (e.g. Xiao et al. [42]). Beam elements (BEAM188
412 [55]) were adopted to simulate columns and shell elements (SHELL181 [55]) were considered
413 for slabs. The finite element model considered those mechanical and geometrical parameters of
414 the experimental test (See Section 2). A linear static analysis was carried out, without considering
415 dynamic amplification (DAF = 1.0). Fig. 19 shows the deformed shape (UY) of the finite element
416 (FE) model, before and after the sudden removal of the column.



417
418 **Fig. 19. UY deformed shape of the structure. Units in m.**

419 Table 3 gives the experimental and numerical results obtained for the displacements (sensor
420 LVDT_P3_11V) and axial force increment of columns P2 and P6. Table 3 provides the DAF
421 computed in this study, as the ratio between the dynamic value obtained experimentally (peak)
422 and the static value obtained numerically from the linear model (i.e. without introducing a
423 dynamic amplification factor). This ratio was computed for displacements (DAF_{LD}) and axial
424 forces (DAF_{LF}), following the definitions used in US DoD [14]. The dynamic axial force in the
425 columns was estimated as the force prior to the column removal (estimated from the linear finite
426 element analysis) plus the load increment obtained during the test after the column removal.

427 **Table 3. Dynamic load amplification factors for deformations and forces.**

Component	Displacement [mm]		DAF _{LD}
	Experimental	Linear static analyses	
P3_11V	48.1	18.2	2.64

Component	Axial force increments [kN]		DAF _{LF} (based on total axial forces)
	Experimental	Linear static analysis	
P2	187	107	1.25
P6	179		1.23
Mean value	183	---	1.24

428

429 As discussed in DoD [14] Annex C (commentary), following the definition above for the
 430 DAFs leads to cases where inertial and nonlinear effects are combined. This leads for example to
 431 a DAF_{LD} larger than 2.0 as shown in Table 3 which could be adopted in DoD as a load increase
 432 factor (LIF) for a linear static analysis. Using a more refined (nonlinear) prediction of the static
 433 displacement would result into DAF_{LD} closer to 2.0 which is the theoretical dynamic amplification
 434 in a 1-DOF linear system for a sudden applied load and no damping. It should be noted that the
 435 LIF in DoD [14] may vary between 2.0 and 3.2 for two-way slabs and slab-column connections,
 436 depending on the ductility which is influenced by the presence of continuity reinforcement in the
 437 slab and the utilisation ratio of the punching shear strength in the connections.

438 The dynamic amplification factor for the axial loads in the columns DAF_{LF} shown in Table 3
 439 were around 1.24. These values are clearly below the value of 2.0 recommended by the DoD [14]
 440 although it is recognised in Annex C of the guidelines that the Dynamic Increase Factor (DIF)
 441 used for nonlinear static solutions is typically less than 2.0. In this case the static value of the axial
 442 loads obtained from the linear analysis is relatively similar to the one obtained in a nonlinear
 443 model and therefore the values of the DAF_{LF} shown in Table 3 are a more truthful reflection of
 444 the dynamic amplification. The values of the dynamic amplification of the load obtained in this
 445 work (DAF_{LF} = 1.24) are also consistent with test results of sudden corner column removal by
 446 Qian and Li [40] in which they report dynamic load increase factors between 1.13 and 1.23. These
 447 results are also comparable with dynamic amplification factors for internal column removal

448 obtained experimentally [47], numerically [9] or theoretically [12] which can vary between 1.6
449 and 1.2.

450

451 **6. Conclusions and future work**

452 This paper describes the study and analysis of an extensive experimental work carried out on
453 a full-scale RC cast-in-place building structure subjected to a sudden corner-column failure
454 scenario. This is the first study of this type (corner-column removal) on a full-scale building
455 expressly built for the purpose subjected to representative loading used in design and provided
456 with a comprehensive monitoring system. After describing the building itself, details are given
457 on the test procedure and the monitoring system used. Real-time strain, displacement and
458 acceleration results and alternative load paths (ALPs) are analysed, and a discussion is included
459 of the overall response of the structure plus the dynamic amplification factors (DAFs). The results
460 obtained allow the following conclusions to be drawn:

- 461 • The structure was able to find effective alternative load paths after the sudden
462 removal of the corner-column, and the dynamic amplification observed did not
463 resulted in extensive damage in the structure.
- 464 • The time-history test results showed that the peak dynamic values were significantly
465 higher than the stabilized residual values after the test. The peaks reached values
466 which were 16%, 71% and 400% higher over the residual values for the vertical
467 displacements, strain in columns and horizontal displacements respectively.
- 468 • The predominant ALPs in the test were the flexural and Vierendeel beam actions,
469 while slab membrane action was not a significant ALP for the case investigated.
- 470 • Dynamic amplification factors (DAFs) were obtained following the definitions in
471 DoD guidelines [14] for load and dynamic increase factors. Regarding the vertical
472 displacements, the values obtained for the load increase factor (combining inertial
473 and nonlinear effects) were around 2.6 which was within the recommended values of

474 DoD [14]. In terms of the axial load amplification, the values obtained for the
475 dynamic increase factor were around 1.24 which is clearly below the standard value
476 of 2.0 used in design. This confirms that adopting a simplified design value of 2.0
477 can lead to unrealistic assessment of damage for column removal situations.

478 The experimental programme presented here will be used in future work towards the
479 validation of dynamic punching shear models for slab-column connections under corner-column
480 removal scenarios. In the near future, the authors will carry out a similar test setup, combined
481 with numerical studies on the influence of masonry infill walls on the test results. The test results
482 shown in this paper can be used for validating future numerical models, verifying improved
483 clauses for robustness in design codes and help towards creating a larger database of full-scale
484 building tests.

485

486 **Acknowledgements**

487 This work was carried out with the support of a 2017 Leonardo Grant for Researchers and
488 Cultural Creators from the BBVA Foundation. The authors would also like to express their
489 gratitude to the *Levantina, Ingeniería y Construcción S.L.* (LIC) company for funding the
490 construction of the building.

491

492 **References**

- 493 [1] Adam JM, Parisi F, Sagaseta J, Lu X. Research and practice on progressive collapse and
494 robustness of building structures in the 21st century. *Eng Struct* 2018;173:122–49.
495 doi:10.1016/j.engstruct.2018.06.082.
- 496 [2] Dat PX, Tan KH. Experimental Response of Beam-Slab Substructures Subject to
497 Penultimate-External Column Removal. *J Struct Eng* 2015;141:1–12.
498 doi:10.1061/(ASCE)ST.1943-541X.0001123.
- 499 [3] Qian K, Li B. Resilience of flat slab structures in different phases of progressive collapse.
500 *ACI Struct J* 2016;113:537–48. doi:10.14359/51688619.
- 501 [4] Fu F. Progressive collapse analysis of high-rise building with 3-D finite element modeling
502 method. *J Constr Steel Res* 2009;65:1269–78. doi:10.1016/j.jcsr.2009.02.001.
- 503 [5] Brunesi E, Nascimbene R, Parisi F, Augenti N. Progressive collapse fragility of reinforced
504 concrete framed structures through incremental dynamic analysis. *Eng Struct*
505 2015;104:65–79. doi:10.1016/j.engstruct.2015.09.024.

- 506 [6] Starossek U. *Progressive Collapse of Structures*. 2nd ed. Thomas Telford Ltd; 2018.
- 507 [7] Russell JM, Sagaseta J, Cormie D, Jones AEK. Historical review of prescriptive design
508 rules for robustness after the collapse of Ronan Point. *Structures* 2019;20:365–73.
509 doi:10.1016/j.istruc.2019.04.011.
- 510 [8] Starossek U. Typology of progressive collapse. *Eng Struct* 2007;29:2302–7.
511 doi:10.1016/J.ENGSTRUCT.2006.11.025.
- 512 [9] Olmati P, Sagaseta J, Cormie D, Jones AEK. Simplified reliability analysis of punching
513 in reinforced concrete flat slab buildings under accidental actions. *Eng Struct*
514 2017;130:83–98. doi:10.1016/j.engstruct.2016.09.061.
- 515 [10] Thiagarajan G, Kadambi A V., Robert S, Johnson CF. Experimental and finite element
516 analysis of doubly reinforced concrete slabs subjected to blast loads. *Int J Impact Eng*
517 2015;75:162–73. doi:10.1016/j.ijimpeng.2014.07.018.
- 518 [11] Pham AT, Tan KH, Yu J. Numerical investigations on static and dynamic responses of
519 reinforced concrete sub-assemblages under progressive collapse. *Eng Struct* 2017;149:2–
520 20. doi:10.1016/j.engstruct.2016.07.042.
- 521 [12] Sagaseta J, Ulaeto N, Russell J. Structural robustness of concrete flat slab structures. *ACI*
522 *Struct J* 2017;315:273–98.
- 523 [13] GSA. General Services Administration. *Progressive collapse analysis and design*
524 *guidelines for new federal office buildings and major organization projects*; 2013.
- 525 [14] DoD. Department of Defense. *Design of buildings to resist progressive collapse (UFC 4-*
526 *023-03)*; 2009.
- 527 [15] EN 1991-1-7. *Eurocode 1: Actions on structures - Part 1-7: General actions - Accidental*
528 *actions*; 2006.
- 529 [16] Qian K, Weng YH, Li B. Impact of two columns missing on dynamic response of RC flat
530 slab structures. *Eng Struct* 2018;177:598–615. doi:10.1016/j.engstruct.2018.10.011.
- 531 [17] Ren P, Li Y, Lu X, Guan H, Zhou Y. Experimental investigation of progressive collapse
532 resistance of one-way reinforced concrete beam-slab substructures under a middle-
533 column-removal scenario. *Eng Struct* 2016;118:28–40.
534 doi:10.1016/j.engstruct.2016.03.051.
- 535 [18] Yi W-J, Kunnath SK, Zhang F-Z, Xiao Y. Large-scale experimental evaluation of building
536 system response to sudden column removal. *Struct. Congr.*, vol. 1, ASCE; 2011, p. 2353–
537 7.
- 538 [19] Tohidi M, Baniotopoulos C. Effect of floor joint design on catenary actions of precast
539 floor slab system. *Eng Struct* 2017;152:274–88. doi:10.1016/j.engstruct.2017.09.017.
- 540 [20] Kang SB, Tan KH. Progressive collapse resistance of precast concrete frames with
541 discontinuous reinforcement in the joint. *J Struct Eng* 2017;143:1–13.
542 doi:10.1061/(ASCE) ST.1943-541X.0001828.
- 543 [21] Al-Salloum YA, Alrubaidi MA, Elsanadedy HM, Almusallam TH, Iqbal RA.
544 Strengthening of precast RC beam-column connections for progressive collapse mitigation
545 using bolted steel plates. *Eng Struct* 2018;161:146–60.
546 doi:10.1016/j.engstruct.2018.02.009.
- 547 [22] Almusallam TH, Elsanadedy HM, Al-Salloum YA, Siddiqui NA, Iqbal RA. Experimental
548 Investigation on Vulnerability of Precast RC Beam-column Joints to Progressive Collapse.
549 *KSCE J Civ Eng* 2018;1–16. doi:10.1007/s12205-018-1518-0.
- 550 [23] Sasani M, Sagioglu S. Gravity load redistribution and progressive collapse resistance of

- 551 20-story reinforced concrete structure following loss of interior column. *ACI Struct J*
552 2010;107:636–44.
- 553 [24] Jian H, Li S, Huanhuan L. Testing and Analysis on Progressive Collapse-Resistance
554 Behavior of RC Frame Substructures under a Side Column Removal Scenario. *J Perform*
555 *Constr Facil* 2016;30:1–7. doi:10.1061/(ASCE)CF.1943-5509.0000873.
- 556 [25] Qian K, Li B. Dynamic and residual behavior of reinforced concrete floors following
557 instantaneous removal of a column. *Eng Struct* 2017;148:175–84.
558 doi:10.1016/j.engstruct.2017.06.059.
- 559 [26] Peng Z, Orton SL, Liu J, Tian Y. Experimental Study of Dynamic Progressive Collapse
560 in Flat-Plate Buildings Subjected to Exterior Column Removal. *J Struct Eng* 2017;143:1–
561 13. doi:10.1061/(ASCE)ST.1943-541X.0001865.
- 562 [27] Kokot S, Anthoine A, Negro P, Solomos G. Static and dynamic analysis of a reinforced
563 concrete flat slab frame building for progressive collapse. *Eng Struct* 2012;40:205–17.
564 doi:10.1016/j.engstruct.2012.02.026.
- 565 [28] Bermejo M, Santos AP, Goicolea JM. Development of Practical Finite Element Models
566 for Collapse of Reinforced Concrete Structures and Experimental Validation. *Shock Vib*
567 2017:1–9. doi:10.1155/2017/4636381.
- 568 [29] Lim NS, Tan KH, Lee CK. Experimental studies of 3D RC substructures under exterior
569 and corner column removal scenarios. *Eng Struct* 2017;150:409–27.
570 doi:10.1016/j.engstruct.2017.07.041.
- 571 [30] Stathas N, Bousias SN, Palios X, Strepelias E, Fardis MN. Tests and Simple Models of
572 RC Frame Subassemblies for Postulated Loss of Column. *J Struct Eng* 2018;144:1–14.
573 doi:10.1061/(ASCE)ST.1943-541X.0001951.
- 574 [31] Qian K, Li B. Performance of Precast Concrete Substructures with Dry Connections to
575 Resist Progressive Collapse. *J Perform Constr Facil* 2018;32:1–14.
576 doi:10.1061/(ASCE)CF.1943-5509.0001147.
- 577 [32] Fu Q, Tan K-H. Numerical study on steel-concrete composite floor systems under corner
578 column removal scenario. *Structures* 2019. doi:10.1016/j.istruc.2019.06.003.
- 579 [33] Kai Q, Li B. Dynamic performance of RC beam-column substructures under the scenario
580 of the loss of a corner column - Experimental results. *Eng Struct* 2012;42:154–67.
581 doi:10.1016/j.engstruct.2012.04.016.
- 582 [34] Gao S, Guo L. Progressive collapse analysis of 20-storey building considering composite
583 action of floor slab. *Int J Steel Struct* 2015;15:447–58. doi:10.1007/s13296-015-6014-5.
- 584 [35] Feng P, Qiang H, Ou X, Qin W, Yang J. Progressive Collapse Resistance of GFRP-
585 Strengthened RC Beam–Slab Subassemblages in a Corner Column–Removal Scenario. *J*
586 *Compos Constr* 2019;23:1–15. doi:10.1061/(ASCE)CC.1943-5614.0000917.
- 587 [36] Zhang H, Shu G, Pan R. Failure Mechanism of Composite Frames Under the Corner
588 Column-Removal Scenario. *J Fail Anal Prev* 2019;19:649–64. doi:10.1007/s11668-019-
589 00644-8.
- 590 [37] Ma F, Gilbert BP, Guan H, Xue H, Lu X, Li Y. Experimental study on the progressive
591 collapse behaviour of RC flat plate substructures subjected to corner column removal
592 scenarios. *Eng Struct* 2019;180:728–41. doi:10.1016/j.engstruct.2018.11.043.
- 593 [38] Qian K, Li B. Performance of Three-Dimensional Reinforced Concrete Beam-Column
594 Substructures under Loss of a Corner Column Scenario. *J Struct Eng* 2013;139:584–94.
595 doi:10.1061/(ASCE)ST.1943-541X.0000630.

- 596 [39] Johnson ES, Meissner JE, Fahnestock LA. Experimental Behavior of a Half-Scale Steel
597 Concrete Composite Floor System Subjected To Column Removal Scenarios. *J Struct Eng*
598 2013;142:1–12. doi:10.1061/(ASCE)ST.1943-541X.0001398.
- 599 [40] Qian K, Li B. Experimental study of drop panel effects on response of reinforced concrete
600 flat slabs after loss of corner column. *ACI Struct J* 2013;845–56.
- 601 [41] Pham AT, Lim NS, Tan KH. Investigations of tensile membrane action in beam-slab
602 systems under progressive collapse subject to different loading configurations and
603 boundary conditions. *Eng Struct* 2017;150:520–36. doi:10.1016/j.engstruct.2017.07.060.
- 604 [42] Xiao Y, Kunnath S, Li FW, Zhao YB, Lew HS, Bao Y. Collapse Test of Three-Story Half-
605 Scale Reinforced Concrete Frame Building. *ACI Struct J* 2015;112:429–38.
606 doi:10.14359/51687746.
- 607 [43] Xiao Y, Zhao YB, Li FW, Kunnath S, Lew HS. Collapse Test of a 3-Story Half-Scale RC
608 Frame Structure. *Struct Congr* 2013:11–9. doi:10.1061/9780784412848.002.
- 609 [44] Zhang L, Zhao H, Wang T, Chen Q. Parametric Analysis on Collapse-resistance
610 Performance of Reinforced-concrete Frame with Specially Shaped Columns Under Loss
611 of a Corner Column. *Open Constr Build Technol J* 2016;10:466–80.
612 doi:10.2174/1874836801610010466.
- 613 [45] Chen Q, Zhao H, Zhang L, Wang T. Progressive collapse resistance of reinforced-concrete
614 frames with specially shaped columns under loss of a corner column. *Mag Concr Res*
615 2015;68:1–15. doi:10.1680/macr.15.00108.
- 616 [46] EN 1990. Eurocode: Basis of structural design; 2002.
- 617 [47] Russell JM, Owen JS, Hajirasouliha I. Experimental investigation on the dynamic
618 response of RC flat slabs after a sudden column loss. *Eng Struct* 2015;99:28–41.
619 doi:10.1016/j.engstruct.2015.04.040.
- 620 [48] EN 1992-1-1. Eurocode 2: Design of concrete structures - Part 1-1: General rules and rules
621 for buildings; 2004.
- 622 [49] EN 1991-1-1. Eurocode 1: Actions on structures. Part 1-1: Densities, self-weight, imposed
623 loads for buildings; 2003.
- 624 [50] Sasani M, Sagioglu S. Progressive Collapse Resistance of Hotel San Diego. *J Struct Eng*
625 2008;134:478–88. doi:10.1061/(ASCE)0733-9445(2008)134:3(478).
- 626 [51] Yi W-J, He Q-F, Xiao Y, Kunnath SK. Experimental Study on Progressive Collapse-
627 Resistant Behavior of Reinforced Concrete Frame Structures. *ACI Struct J* 2008;105:433–
628 9. doi:10.14359/19857.
- 629 [52] Black MS. Ultimate Strength Study of Two-Way Concrete Slabs. *ASCE J Struct Div*
630 1975;101:311–24.
- 631 [53] Rankin GIB, Long AE. Arching action strength enhancement in laterally-restrained slab
632 strips. *Proc Inst Civ Eng - Struct Build* 1997;122:461–7. doi:10.1680/istbu.1997.29834.
- 633 [54] Park R, Gamble WL. Reinforced Concrete Slabs. 2nd ed. New York: John Wiley & Sons,
634 Inc; 2000.
- 635 [55] ANSYS 15.0. Theory reference. ANSYS Inc. 2014.
- 636
- 637